Quantum-Dot Single-Photon Sources for Entanglement Enhanced Interferometry

M. Müller,[1,*] H. Vural,[1] C. Schneider,[2] A. Rastelli,[3] O. G. Schmidt,[4] S. Höfling,[2,5] and P. Michler[1,†]

[1]*Institut für Halbleiteroptik und Funktionelle Grenzflächen, Center for Integrated Quantum Science and Technology (IQST) and SCoPE,
Universität Stuttgart, Allmandring 3, 70569 Stuttgart, Germany*
[2]*Technische Physik and Wilhelm Conrad Röntgen Research Center for Complex Material Systems, Physikalisches Institut,
Universität Würzburg, Am Hubland, 97074 Würzburg, Germany*
[3]*Institute of Semiconductor and Solid State Physics, Johannes Kepler University Linz, Altenbergerstrasse 69, 4040 Linz, Austria*
[4]*Institute for Integrative Nanosciences, IFW Dresden, Helmholtzstr. 20, 01069 Dresden, Germany*
[5]*SUPA, School of Physics and Astronomy, University of St. Andrews KY 16 9SS, Scotland, United Kingdom*

Multiphoton entangled states such as "N00N states" have attracted a lot of attention because of their possible application in high-precision, quantum enhanced phase determination. So far, N00N states have been generated in spontaneous parametric down-conversion processes and by mixing quantum and classical light on a beam splitter. Here, in contrast, we demonstrate superresolving phase measurements based on two-photon N00N states generated by quantum dot single-photon sources making use of the Hong-Ou-Mandel effect on a beam splitter. By means of pulsed resonance fluorescence of a charged exciton state, we achieve, in postselection, a quantum enhanced improvement of the precision in phase uncertainty, higher than prescribed by the standard quantum limit. An analytical description of the measurement scheme is provided, reflecting requirements, capability, and restraints of single-photon emitters in optical quantum metrology. Our results point toward the realization of a real-world quantum sensor in the near future.

Optical quantum metrology provides a route to enhance sensing applications by utilizing, e.g., nonclassical states of light [1–4]. For many photonic sensing schemes, a general task is measuring a phase φ with a precision $\Delta\varphi$. Here, the maximum achievable precision is subject to several limitations. The most fundamental boundary, based on a quantum mechanical uncertainty principle, is the so-called Heisenberg limit (HL). It relates the error of phase estimation $\Delta\varphi$ with the photon number N used for the measurement to $\Delta\varphi_{HL} = 1/N$ [1]. However, as a consequence of the central limit theorem of statistics, the phase determination of interferometric sensing schemes utilizing classical light states is restricted to the so-called standard quantum limit (SQL), scaling with $\Delta\varphi_{SQL} = 1/\sqrt{N}$ in absence of losses. On the contrary, a maximally path-entangled multiphoton state, a so-called N00N state $|\Phi\rangle_N = (1/\sqrt{2})(|N,0\rangle + |0,N\rangle)$, acquires a phase at a rate N times as fast as classical light. As a consequence, the frequency of the obtained interference fringe pattern is increased by a factor of N, referred to as superresolution [5,6]. If the contrast of the oscillations exceeds the threshold $C_{th} = 1/\sqrt{N}$, the regime of supersensitivity [7,8] is reached. In this case, the entanglement allows for quantum enhanced phase measurements outperforming the SQL and approaching the fundamental Heisenberg limit. Practical imperfections, such as loss, decoherence, state preparation and detector inefficiency can degrade this quantum enhancement. Therefore, a careful resource accounting is necessary to judge real-world enhancement [9].

So far, various schemes for generating N00N states have been realized and phase superresolution has been demonstrated in a number of studies [10–14]. Phase supersensitivity, or beating the SQL, has been demonstrated with four entangled photons using postselected state projection to study the N00N component of various initial N-photon states [15]. The largest N00N state generated to date contained five photons by mixing quantum and classical light [16].

Up to now, the majority of multiphoton interference realizations concerning path-entangled photon states relied on parametric down-conversion photon sources, partially in heralding operation modes. In this Letter, we focus on single semiconductor quantum dots (QD) and investigate their potential as single-photon sources in an optical quantum metrology scheme. These emitters of nonclassical light can be operated with high efficiency and brightness [17,18] to generate, e.g., entangled photon states [19]. At the same time, compact on-chip implementation is feasible [20,21]. Recently, off- and on-chip implementations of an entangling CNOT gate operating with quantum dot micropillar single-photon sources have been demonstrated [22,23]. Biphotonic interference of photons generated by a semiconductor quantum dot, however, based on entanglement in the polarization degree of freedom [24,25], has been used to demonstrate phase superresolution [26]. Just recently, the same effect with path-entangled photon states from a quantum dot was realized in an on-chip experiment [14]. However, the regime of phase supersensitivity has not been attained using a deterministic single-photon emitter, so far.

Here, we present an experimental realization of the generation of two-photon N00N states by using the radiative recombination of excitonic states in a single semiconductor quantum dot. Such a single quantum emitter is coherently

and resonantly driven by employing two different excitation schemes on two different samples. In the first one, a biexciton state of the QD is deterministically prepared via a two-photon excitation process [27–30], resulting in the emission of a pair of single-photons from the biexciton (XX)—exciton (X)—ground-state (G) cascade [Fig. 1(a)]. In the second one, a charged exciton, a so-called trion (T) is excited via a pulsed single-photon resonance-fluorescence scheme [Fig. 1(b)]. Both methods lead to the deterministic generation of pure single photons of high optical and quantum-optical quality (see Supplemental Material [32]), which allow for the production of two-photon N00N states and the observation of phase superresolution, and even phase supersensitivity for the T state.

The experimental setup is illustrated in Figs. 1(c) and 1(d). Applying a double pulse excitation scheme on the QD, two consecutively emitted photons (either X, XX, or T, respectively) with a time separation Δt are launched into an unbalanced Mach-Zehnder interferometer (MZI), consisting of beam splitters BS1 and BS2. Here, the initial time separation between the photons can be compensated by the delay Δt in the MZI, so that they impinge simultaneously onto BS2 from different input ports (red spheres) [31]. At the interference point (which we denote as BS2′), the Hong-Ou-Mandel (HOM) effect [34] for identical bosonic particles causes then the generation of the two-particle path-entangled state

$$|\Phi\rangle_2 = (|2\rangle \otimes |0\rangle + |0\rangle \otimes |2\rangle)/\sqrt{2}$$
$$= (|20\rangle + |02\rangle)/\sqrt{2}, \tag{1}$$

which implies that both photons can only be detected together in either one of the two exit ports of BS2′ (blue spheres). The biphotonic N00N state evolves by passing through the Sagnac type double-path interferometer in which a relative phase $e^{i\varphi}$ is acquired in one mode, introduced by turning an ordinary glass plate. Here, the chosen Sagnac interferometer design serves as an intrinsically phase stable realization of a balanced MZI consisting of BS2′ and BS2″ [see Figs. 1(c) and 1(d)], with BS2″ being the position on BS2 where photons meet after traveling the interferometer. Because of the nonclassical nature, the photonic state picks up the phase $N = 2$ times faster than a coherent state would do [35]:

$$|\Phi\rangle_2 \xrightarrow{\varphi} (|20\rangle + e^{i2\varphi}|02\rangle)/\sqrt{2}. \tag{2}$$

The coherence of this state is determined by measuring the phase-dependent coincidence probability after BS2″ on detector D1 and D2:

$$\mathcal{P}_{D1,D2} = [1 + \cos(2\varphi)]/2. \tag{3}$$

Thus, an oscillating behavior with a frequency according to twice the imprinted phase is expected in the intensity autocorrelation measurement. Since the two consecutive single photons emitted by the QD can arrive at BS2′ with delays of 0, $\pm\Delta t$ and $\pm 2\Delta t$ with $\Delta t = 4.4$ ns, we expect clusters of five peaks separated by the pump laser repetition period (13.1 ns) in the measured coincidence histogram (cluster $Cl_{1,2,3}$ in Fig. 2). Because of the large spacing between neighboring peaks of a single excitation cycle, the two outermost peaks of each side of the cluster temporally overlap with the corresponding peaks from the previous or successive cluster (ΣCl_i in Fig. 2). However, the central peak, which reflects the desired situation when both photons arrive at the same time at beam splitter BS2′ is well resolved and not affected by any overlap of the Δt time separation between the pulses. A selection of measurements
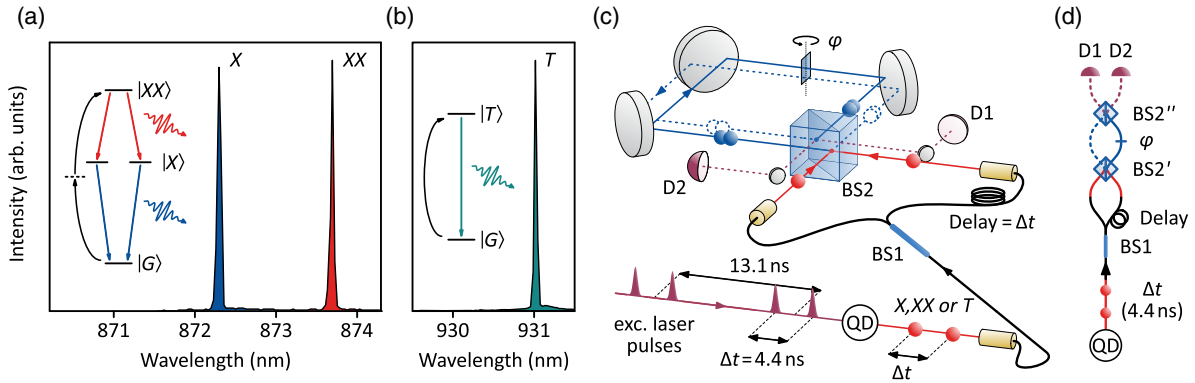

FIG. 1. (a) Two-photon excitation scheme via a virtual state (dashed line) and the cascaded emission of a pair of biexciton (XX) and exciton (X) single-photons with corresponding spectrum [only one of the two available recombination paths $((|\uparrow\Downarrow, \downarrow\Uparrow\rangle_{XX} \to |\uparrow\Downarrow\rangle_X$ or $|\downarrow\Uparrow\rangle_Y \to |G\rangle))$ is considered in the conducted experiment]. (b) Pulsed resonance-fluorescence of a charged exciton (T) in a quantum dot with corresponding spectrum. (c) Intrinsically phase-stable double-path Sagnac interferometer [15] with laser excitation scheme. First, beam splitter 2 (BS2) serves as the second part of an unbalanced MZI [with beam splitter 1 (BS1)] to generate the $|\Phi\rangle_2 = (|20\rangle + |02\rangle)/\sqrt{2}$ state by exploiting two-photon interference at a position BS2′ [31]. The path-entanglement is then probed via phase-dependent autocorrelation measurements again on BS2, on a second interference position BS2″. By rotating a phase plate (an ordinary glass plate in our case) in one of the arms, the relative phase difference φ between the two paths (blue dotted and solid lines) is varied. (d) Unfolded scheme of the photon path in the Sagnac interferometer.
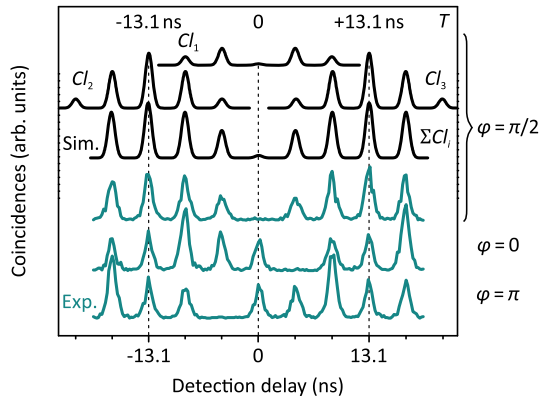
FIG. 2.   Coincidence histogram simulation and data for the trion line. The black lines Cl_1, Cl_2, and Cl_3 show the expected five peak clusters which are separated by the laser repetition period of 13.1 ns for a phase shift of $\varphi = \pi/2$. In this special case the outcome is the same as for a typical Hong-Ou-Mandel experiment. The sum of these clusters (ΣCl_i) displays the expected histogram which is in very good agreement with the measurement (top green line). The two green lines for phase shifts of $\varphi = 0$ and $\varphi = \pi$ reflect measurement situations of constructive biphotonic interference.

using photons from the T decay is depicted in the lower part of Fig. 2 (green solid lines) for three distinct phase settings. By adjusting the relative phase to $\varphi = \pi/2$, the intensity distribution in the output modes of BS2′ and BS2″ are identical and correspond to the outcome of a typical two-photon interference measurement. The almost vanishing coincidence peak at zero detection delay indicates a high degree of indistinguishability of consecutive photons emitted by the QD. As discussed later, the ability to generate these pure, nearly transform-limited single photons essentially defines the coherence of the biphotonic N00N state. In contrary, setting the relative phase φ between the paths to 0 or π leads to constructive interference in the coincidence peak. (Further details about the occurrence and oscillating behavior of the coincidence peaks at nonzero detection delay as well as a complete theoretical analysis can be found in the Supplemental Material [36]).

The full phase dependency of the intensity correlation is shown in Fig. 3. In the first row, single-photon interference with a frequency of ν_i with $i = \{X, XX, T\}$ is observed by blocking one input of BS2′ and using only one of the

TABLE I.   Summarized measurement results. $g^{(2)}(0)$ gives the multiphoton emission probability, η the spatial beam overlap of the entire Mach-Zehnder interferometer, V_{HOM} the two-photon interference visibility, and $C_{N=i}$ with $i = \{1, 2\}$ the N00N state interference visibility.

	$g^{(2)}(0)$	η	V_{HOM}	$C_{N=1}$	$C_{N=2}$
X	0.004(2)	0.91(1)	0.43(4)	0.91(1)	0.44(1)
XX	0.003(2)	0.88(1)	0.76(3)	0.90(1)	0.54(1)
T	0.003(3)	0.99(1)	0.92(4)	0.99(1)	0.87(2)

two detectors. The respective fringe contrasts of $C_{1,X} = 0.91(1)$, $C_{1,XX} = 0.90(1)$, and $C_{1,T} = 0.99(1)$ confirm the viability of the interferometer, that is, a sufficient mode overlap on beam splitter BS2″. In the next step, the blocked path is reopened to enable the generation of N00N states with $N = 2$ through the previously described Hong-Ou-Mandel effect. The phase-dependent postselected coincidence rates between both detectors are displayed in the second row of Fig. 3. Highly pronounced oscillations with twice the single-photon frequency are a strong indication for the successful generation of biphotonic path-entangled states. However, a strong deviation in the amplitude and the contrast between the experiments of the three different single-photon input states X, XX, and T is obvious.

To get more insight into the underlying processes, the common beam splitter and phase transformations were applied to the individual input states to model the data. The probability to measure a coincidence event can then be expressed as a function of two additional parameters, the two-photon interference visibility V_{HOM} and the spatial mode overlap of the entire interferometer $\eta = \sqrt{\eta'\eta''}$ with overlaps η' on BS2′ and η'' on BS2″, respectively:

$$\mathcal{P}_{\text{D1,D2}}^{\text{exp}} = \frac{1}{4}[2 + \eta^2(1 - \eta^2 V_{\text{HOM}})$$
$$+ \eta^2(1 + \eta^2 V_{\text{HOM}})\cos(2\varphi)]. \quad (4)$$

For ideal experimental conditions and entirely identical photons ($\eta = V_{\text{HOM}} = 1$), this relation reduces to Eq. (3), giving rise to the expected oscillations with maximum contrast. The contrast is defined by $(I_{\max} - I_{\min})/(I_{\max} + I_{\min})$ with $I_{\max}$ the maximum and $I_{\min}$ the minimum signal of the oscillation. As pointed out before, for distinct phase settings of odd integer multiples of $\pi/2$, the measurement corresponds to a Hong-Ou-Mandel type two-photon interference experiment. These are the data points at the minima of the oscillations; hence, the two-photon output probability is the limiting factor for $I_{\min}$. In contrast, the influence of η is related to the maximum values of the oscillations $I_{\max}$ of the N00N state measurement, and is also reflected in the visibility of the single-photon oscillations.

Applying the model to the data, N00N state fringe contrasts of $C_{2,X} = 0.44(1)$ and $C_{2,XX} = 0.54(1)$ are extracted. The X and XX photons, generated by two-photon excitation, are strongly limited by the rather low mode overlap of the measurement device. This becomes crucial especially for the XX photons, which show an adequate Hong-Ou-Mandel visibility of $V_{\text{HOM},XX} = 0.76(3)$ to outperform the SQL. Here, a threshold mode overlap of $\eta_{\text{th},XX} = 0.97$ would be sufficient to generate the required N00N state contrast. The emitted photons from the X state suffer from a time jitter induced by the XX recombination lifetime, resulting in an insufficient Hong-Ou-Mandel visibility of $V_{\text{HOM},X} = 0.43(4)$.

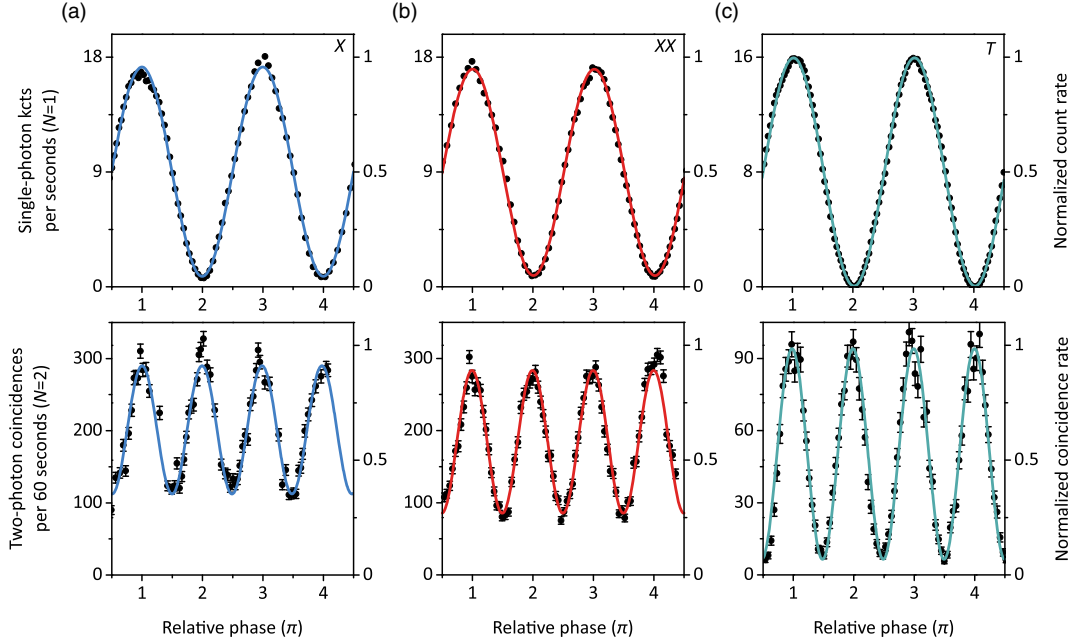In a subsequent set of experiments a spatial mode cleaner, realized by implementing single-mode fibers

FIG. 3.   Phase-dependent single-photon count rates (top row) and biphotonic coincidence rates (bottom row) for (a) X, (b) XX, and (c) T. Phase superresolution is achieved in all three cases. Insufficient two-photon interference visibility (e.g. X), or inadequate spatial mode overlap (e.g. XX) can prevent supersensitivity. On the contrary, the measurement using photons from the T decay shows an improvement of phase precision beyond the standard quantum limit (see main text). Error bars represent the statistical error of the coincidence measurement.

(coupling efficiency > 0.95) in the detection path, drastically increases the single-photon oscillation contrast to near unity [top of Fig. 3(c)]. Additionally, the pulsed resonant excitation of a charged exciton T, realized by a confocal setup geometry including cross-polarization of the scattered laser light, revealed exceptionally high two-photon interference visibility of $V_{\mathrm{HOM},T} = 0.92(4)$. The reason for the successful generation of these nearly transform-limited photons [38–40] emitted by the resonantly pumped T state is mainly attributed to the high purity of the sample achieved by the growth mode [32]. In combination, the increased mode overlap and high two-photon interference visibility result in a contrast visibility of the biphotonic N00N state measurement of $C_{2,T} = 0.87(1)$, exceeding the threshold given by the SQL ($C_{\mathrm{th}} = 0.71$). A summary of the obtained results is given in Table I.

Phase superresolution can also be realized by utilizing classical light sources, and is no evidence for the generation of a nonclassical N00N state [41]. Quite the contrary, in a perfect setup ($\eta = 1$) single photons with vanishing two-photon interference visibility ($V_{\mathrm{HOM}} = 0$) would still show oscillations with doubled frequency, however limited to an oscillation visibility of $1/3$. The exploitation of entanglement comes into effect only when the contrast surpasses the classical limit of $C_{\mathrm{th}} = 1/\sqrt{N}$, in which case phase supersensitive measurements are theoretically feasible. While fulfilling this requirement unambiguously proves the nonclassical nature of the used light states, it does not make a statement about the measurement precision compared to a scheme using classical light in the context of resource

counting. By taking into account real world imperfections such as losses and nonunity efficiencies, the threshold to beat the classical limit, which is then given by the so-called standard interferometric limit (SIL), has to be redefined [9,42]. Including these effects, the redefined threshold is given by $C_{\mathrm{th}} = \sqrt{1/\xi_p(\xi_i\xi_d)^{N-1}N}$, with the N00N state generation efficiency ξ_p, the interferometer transmissivity ξ_i (here, 0.90) and detection probability ξ_d (here, 0.45). Here, the classical limit is determined by considering a coherent state, experiencing the same losses ξ_i and detection efficiencies ξ_d. To surpass this contrast threshold, for a N00N state, $C_{\mathrm{th}} < 1$ as well as $C_N > C_{\mathrm{th}}$ must be fulfilled, putting stringent bounds on source, setup, and detection performance. To our knowledge, there has been no experiment accomplishing these conditions at the same time. Because of the sample design which is not optimized for high extraction efficiencies (~ 0.01), and the nonperfect two-photon interference visibility as well as the factor of 0.25 due to the setup design (only in one out of four cases two consecutive emitted photons impinge on BS2' from opposite sides) the absolute N00N state generation probability in the scheme presented in this work scales with $\xi_p \sim 10^{-5}$, ruling out any attempt for nonpostselected supersensitive phase estimation. Here, the setup design inefficiency can be circumvented either by a simple fast optical switch or a more challenging approach of utilizing two remote QD sources. To reveal the fundamental potential of QDs as photon sources in such an interferometric scheme, we may assume state-of-the-art performance

concerning indistinguishability (0.99 [43–45]), photon extraction (0.80 [17,18]), as well as cutting edge detector efficiencies (0.95 [46]). By doing so, we obtain $C_{th} = 0.96$ as well as $C_{N=2}^{opt} = 0.96$, which shows that real-world quantum sensors based on semiconductor quantum dots come into close reach of entanglement enhanced precision measurements with already available technologies [36].

From a practical point of view, such a sensor has the great benefit of being able to be operated at high overall single-photon rates (up to GHz), which is an essential precondition for fast sensing applications, though putting an additional requirement on the potential sources. Also schemes for producing higher $(N > 2)$ nonclassical N-photon states using N independently generated photons will largely profit from on-demand sources due to an advantageous scaling behavior [47,48].

In summary, we have demonstrated phase superresolution and phase supersensitivity in postselection of biphotonic N00N states by utilizing photons emitted from a semiconductor quantum dot. We provided an analytical description of the interferometric scheme and could thereby fully reproduce and verify the measured data. In a treatment taking into account real-world imperfections we have determined the high potential and limitations of such a device for future applications.

---

[*] m.mueller@ihfg.uni-stuttgart.de
[†] p.michler@ihfg.uni-stuttgart.de

[1] V. Giovannetti, S. Lloyd, and L. Maccone, Phys. Rev. Lett. **96**, 010401 (2006).

[2] J. P. Dowling, Contemp. Phys. **49**, 125 (2008).

[3] M. Kacprowicz, R. Demkowicz-Dobrzański, W. Wasilewski, K. Banaszek, and I. A. Walmsley, Nat. Photonics **4**, 357 (2010).

[4] M. A. Taylor and W. P. Bowen, Phys. Rep. **615**, 1 (2016).

[5] J. Jacobson, G. Björk, I. Chuang, and Y. Yamamoto, Phys. Rev. Lett. **74**, 4835 (1995).

[6] E. J. S. Fonseca, C. H. Monken, and S. Pádua, Phys. Rev. Lett. **82**, 2868 (1999).

[7] C. M. Caves, Phys. Rev. D **23**, 1693 (1981).

[8] A. Kuzmich and L. Mandel, J. Eur. Opt. Soc. B **10**, 493 (1998).

[9] N. Thomas-Peter, B. J. Smith, A. Datta, L. Zhang, U. Dorner, and I. A. Walmsley, Phys. Rev. Lett. **107**, 113603 (2011).

[10] J. G. Rarity, P. R. Tapster, E. Jakeman, T. Larchuk, R. A. Campos, M. C. Teich, and B. E. A. Saleh, Phys. Rev. Lett. **65**, 1348 (1990).

[11] D. Bouwmeester, Nature (London) **429**, 139 (2004).

[12] P. Walther, J.-W. Pan, M. Aspelmeyer, R. Ursin, S. Gasparoni, and A. Zeilinger, Nature (London) **429**, 158 (2004).

[13] M. W. Mitchell, J. S. Lundeen, and A. M. Steinberg, Nature (London) **429**, 161 (2004).

[14] A. J. Bennett, J. P. Lee, D. J. P. Ellis, T. Meany, E. Murray, F. F. Floether, J. P. Griffiths, I. Farrer, D. A. Ritchie, and A. J. Shields, Sci. Adv. **2**, e1501256 (2016).

[15] T. Nagata, R. Okamoto, J. L. O'Brien, K. Sasaki, and S. Takeuchi, Science **316**, 726 (2007).

[16] I. Afek, O. Ambar, and Y. Silberberg, Science **328**, 879 (2010).

[17] J. Claudon, J. Bleuse, N. S. Malik, M. Bazin, P. Jaffrennou, N. Gregersen, C. Sauvan, P. Lalanne, and J.-M. Gérard, Nat. Photonics **4**, 174 (2010).

[18] O. Gazzano, S. Michaelis de Vasconcellos, C. Arnold, A. Nowak, E. Galopin, I. Sagnes, L. Lanco, A. Lemaître, and P. Senellart, Nat. Commun. **4**, 1425 (2013).

[19] A. Dousse, J. Suffczyński, A. Beveratos, O. Krebs, A. Lemaître, I. Sagnes, J. Bloch, P. Voisin, and P. Senellart, Nature (London) **466**, 217 (2010).

[20] M. Arcari, I. Söllner, A. Javadi, S. Lindskov Hansen, S. Mahmoodian, J. Liu, H. Thyrrestrup, E. H. Lee, J. D. Song, S. Stobbe, and P. Lodahl, Phys. Rev. Lett. **113**, 093603 (2014).

[21] U. Rengstl, M. Schwartz, T. Herzog, F. Hargart, M. Paul, S. L. Portalupi, M. Jetter, and P. Michler, Appl. Phys. Lett. **107**, 021101 (2015).

[22] M. A. Pooley, D. J. P. Ellis, R. B. Patel, A. J. Bennett, K. H. A. Chan, I. Farrer, D. A. Ritchie, and A. J. Shields, Appl. Phys. Lett. **100**, 211103 (2012).

[23] O. Gazzano, M. P. Almeida, A. K. Nowak, S. L. Portalupi, A. Lemaître, I. Sagnes, A. G. White, and P. Senellart, Phys. Rev. Lett. **110**, 250501 (2013).

[24] R. J. Young, R. M. Stevenson, P. Atkinson, K. Cooper, D. A. Ritchie, and A. J. Shields, New J. Phys. **8**, 29 (2006).

[25] N. Akopian, N. H. Lindner, E. Poem, Y. Berlatzky, J. Avron, D. Gershoni, B. D. Gerardot, and P. M. Petroff, Phys. Rev. Lett. **96**, 130501 (2006).

[26] R. M. Stevenson, A. J. Hudson, R. J. Young, P. Atkinson, K. Cooper, D. A. Ritchie, and A. J. Shields, Opt. Express **15**, 6507 (2007).

[27] K. Brunner, G. Abstreiter, G. Böhm, G. Tränkle, and G. Weimann, Phys. Rev. Lett. **73**, 1138 (1994).

[28] S. Stufler, P. Machnikowski, P. Ester, M. Bichler, V. M. Axt, T. Kuhn, and A. Zrenner, Phys. Rev. B **73**, 125304 (2006).

[29] H. Jayakumar, A. Predojević, T. Huber, T. Kauten, G. S. Solomon, and G. Weihs, Phys. Rev. Lett. **110**, 135505 (2013).

[30] M. Müller, S. Bounouar, K. D. Jöns, M. Glässl, and P. Michler, Nat. Photonics **8**, 224 (2014).

[31] C. Santori, D. Fattal, J. Vučković, G. S. Solomon, and Y. Yamamoto, Nature (London) **419**, 594 (2002).

[32] See Supplemental Material at http://link.aps.org/supplemental/10.1103/PhysRevLett.118.257402, which includes Ref. [33], for details on the sample characteristics and growth technique.

[33] S. Maier, P. Gold, A. Forchel, N. Gregersen, J. Mørk, S. Höfling, C. Schneider, and M. Kamp, Opt. Express **22**, 8136 (2014).

[34] C. K. Hong, Z. Y. Ou, and L. Mandel, Phys. Rev. Lett. **59**, 2044 (1987).

[35] C. Gerry and P. Knight, Introductory Quantum Optics (Cambridge University Press, Cambridge, England, 2005).

[36] See Supplemental Material at http://link.aps.org/supplemental/10.1103/PhysRevLett.118.257402, which includes Ref. [37], for details on the calculations.

[37] S. L. Braunstein and C. M. Caves, Phys. Rev. Lett. **72**, 3439 (1994).

[38] Y.-M. He, Y. He, Y.-J. Wei, D. Wu, M. Atatüre, C. Schneider, S. Höfling, M. Kamp, C.-Y. Lu, and J.-W. Pan, Nat. Nanotechnol. **8**, 213 (2013).

[39] A. V. Kuhlmann, J. H. Prechtel, J. Houel, A. Ludwig, D. Reuter, A. D. Wieck, and R. J. Warburton, Nat. Commun. **6**, 8204 (2015).

[40] P. Androvitsaneas, A. B. Young, C. Schneider, S. Maier, M. Kamp, S. Höfling, S. Knauer, E. Harbord, C. Y. Hu, J. G. Rarity, and R. Oulton, Phys. Rev. B **93**, 241409 (2016).

[41] K. J. Resch, K. L. Pregnell, R. Prevedel, A. Gilchrist, G. J. Pryde, J. L. O'Brien, and A. G. White, Phys. Rev. Lett. **98**, 223601 (2007).

[42] U. Dorner, R. Demkowicz-Dobrzanski, B. J. Smith, J. S. Lundeen, W. Wasilewski, K. Banaszek, and I. A. Walmsley, Phys. Rev. Lett. **102**, 040403 (2009).

[43] X. Ding, Y. He, Z.-C. Duan, N. Gregersen, M.-C. Chen, S. Unsleber, S. Maier, C. Schneider, M. Kamp, S. Höfling, C.-Y. Lu, and J.-W. Pan, Phys. Rev. Lett. **116**, 020401 (2016).

[44] N. Somaschi, V. Giesz, L. De Santis, J. C. Loredo, M. P. Almeida, G. Hornecker, S. L. Portalupi, T. Grange, C. Antón, J. Demory, C. Gómez, I. Sagnes, N. D. Lanzillotti-Kimura, A. Lemaítre, A. Auffeves, A. G. White, L. Lanco, and P. Senellart, Nat. Photonics **10**, 340 (2016).

[45] S. Unsleber, Y.-M. He, S. Gerhardt, S. Maier, C.-Y. Lu, J.-W. Pan, N. Gregersen, M. Kamp, C. Schneider, and S. Höfling, Opt. Express **24**, 8539 (2016).

[46] A. E. Lita, A. J. Miller, and S. W. Nam, Opt. Express **16**, 3032 (2008).

[47] H. F. Hofmann, Phys. Rev. A **70**, 023812 (2004).

[48] See Supplemental Material at http://link.aps.org/supplemental/10.1103/PhysRevLett.118.257402, which includes Ref. [49], for details.

[49] B. Bell, S. Kannan, A. McMillan, A. S. Clark, W. J. Wadsworth, and J. G. Rarity, Phys. Rev. Lett. **111**, 093603 (2013).